Universal spray-deposition process for scalable, high performance and stable organic electrochemical transistors

*Xihu Wu, Abhijith Surendran, Maximilian Moser, Shuai Chen, Bening Tirta Muhammad, Iuliana Petruta Maria, Iain McCulloch and Wei Lin Leong**

X. Wu, A. Surendran, Dr. S. Chen, B. T. Muhammad, Prof. W. L. Leong
School of Electrical Electronic Engineering
Nanyang Technological University
50 Nanyang Avenue, Singapore 639798, Singapore
E-mail: wlleong@ntu.edu.sg

M. Moser, I.P. Maria, Prof. I. McCulloch
Department of Chemistry,
Imperial College London, London, SW7 2AX, UK

B. T. Muhammad
Interdisciplinary Graduate School, Nanyang Technological University, 50 Nanyang Avenue, Singapore 639798, Singapore

Prof. I. McCulloch
King Abdullah University of Science and Technology (KAUST), Physical Sciences and Engineering Division, KAUST Solar Center (KSC), Thuwal 23955-6900, Saudi Arabia

KEYWORDS: spray-deposition, organic electrochemical transistors, facile patterning technique, bioelectronics, flexible electronics

Abstract

Organic electrochemical transistors (OECTs) with high transconductance and good operating stability in an aqueous environment are receiving substantial attention as promising ion-to-electron transducers for bioelectronics. However, to date, in most of the reported OECTs, the fabrication procedures have been devoted to the spin coating processes which may nullify the advantages of large-area and scalable manufacturing. In addition, conventional microfabrication and photolithography techniques are complicated or incompatible with various nonplanar flexible and curved substrates. Herein, we demonstrate a facile patterning method via spray-deposition to fabricate ionic liquid doped poly(3,4-ethylenedioxythiophene):poly(styrenesulfonate) (PEDOT:PSS)-based OECTs, with a high

peak transconductance of 12.9 mS and high device stability over 4000 switching cycles. More importantly, this facile technique makes it possible to fabricate high-performance OECTs on versatile substrates with different textures and form factors such as thin permeable membranes, flexible plastic sheets, hydrophobic elastomers and rough textiles. Overall, the results highlight the spray-deposition technique as a convenient route to prepare high performing OECTs and will contribute to the translation of OECTs into real-world applications.

INTRODUCTION

Organic electrochemical transistors (OECTs) with high transconductance (> 1 mS) and good operating stability in an aqueous environment are receiving substantial attention as a promising ion-to-electron transducer for bioelectronics.[1–5] OECT-based bioelectronic devices have been successfully used for sensing glucose,[6] DNA[7,8] and hormones,[9] owing to their high sensitivity and low operation voltages. Specifically, the conducting polymers used in OECTs exhibit low impedance in physiological environment and thus govern a stable electrophysiological signal recording for biological diagnosis and therapy.[10,11] Additionally, their simple device structure allows the potential for large-area electronics using simple printing methods such as ink-jet printing and screen-printing.[12–16]

In OECTs, poly(3,4-ethylenedioxythiophene):poly(styrenesulfonate) (PEDOT:PSS), a mixed ion-electron conducting polymer, is the most widely employed active material. The operation of OECTs involves the doping and de-doping of the organic conjugated polymer coupled with ion intercalation under the application of a gate voltage. The OECT performances are influenced by the combination of electronic transport in PEDOT chains and ion penetration from the electrolyte into active channel. A solvent additive, ethylene glycol (EG), is commonly utilised to improve the PEDOT domains for better connectivity and transport.[17–19] In earlier work, we demonstrated how the addition of an ionic liquid into PEDOT:PSS allows for a more closely packed order of PEDOT units and fibrillar morphology to facilitate a better pathway for hole transport and enhanced ion penetration.[20] However, to date, in most of the reported OECTs, the fabrication procedures have been devoted to the spin coating processes which may nullify the advantages of large-area and scalable manufacturing. The state-of-the-art fabrication processes for OECTs also rely heavily on costly and complicated photolithography techniques to achieve a well-patterned active channel for high-performance devices and to avoid parasitic effects.[1,21,22] A well-

patterned polymer channel is desired since the OECT operation is through a volumetric doping/de-doping effect and therefore the channel geometry (W*d/L) plays a critical role in determining the electrical performance.[21,23] Unfortunately, the conventional microfabrication photolithography techniques also require the assistance of diverse organic solvents such as acetone, toluene, or photoresist developers which can lead to damage or delamination of the organic channel layer.

One promising alternative deposition technique is spray-coating, which involves the formation of active layers by sprayed droplets deposition.[24–26] The spray-coating process also allows lower material losses during deposition and is easily scalable for large area electronics.[27–29] Another advantage of spray-coating is that it enables the deposition of films on non-flat surfaces. This is particularly useful for making OECTs for wearable bioelectronics and transient electronics which require versatile substrates with different textures and form factors such as thin permeable membranes, flexible plastic sheets, hydrophobic elastomers, porous paper and rough textiles.[2,30] Among the spray deposition techniques, air brush spray methods are inexpensive and allow high throughput.[31] However, there are very few reports on the fabrication of OECTs by the spray-coating method,[18,25] and in particular, the use of air brush spray methods for PEDOT:PSS deposition for OECT channel.

Herein, we successfully demonstrate a facile air brush spray deposition technique to fabricate ionic liquid doped PEDOT:PSS-based OECTs with high transconductance and excellent stability. The spray-deposition technique enables a one-step preparation of a well-confined PEDOT:PSS channel through the use of a stencil mask. Notably, the spray deposited OECT presents excellent electrical performance, with a high peak transconductance of 12.9 mS (V_D = -0.6 V, W/L = 1000 μm/250 μm, channel thickness, d = ~ 400 nm) and excellent stability during pulsed measurements with over 4000 cycles of

continuous operation. Furthermore, we observe a remarkable ambient stability over six months storage in ambient atmosphere. Most importantly, this organic solvent-free patterning technique makes it possible to fabricate high performance OECTs on a number of diverse nonplanar flexible substrates. In particular, we show that high performing OECTs can be fabricated on biodegradable flexible substrates based on ethyl-cellulose and natural leaf, wearable type substrates based on commercial adhesive bandages and deformable elastic substrates based on a polystyrene-block-poly(ethylene-ran-butylene)-block-polystyrene (SEBS) elastomer. These substrates either have rough surfaces, are thin (5 – 28 μm thick) and/or are vulnerable to commonly used organic solvents such as acetone and toluene, thus meaning that it is challenging to fabricate a well-confined active channel using traditional deposition process or patterning techniques. Using these substrates, the spray-deposited OECTs maintained high electrical performances with a transconductance of 3.7 – 7.4 mS at V_G = 0 V and an on/off ratio of ~5×10^2. To the best of our knowledge, this is the first spray-deposited PEDOT:PSS channels for OECTs on a number of diverse substrates with high electrical performance and superior stability. Additionally, we present an inverter based entirely on OECTs with a high gain of ~18 by combining a PEDOT:PSS based OECT (depletion-mode) and a glycolated thiophene polymer based OECT (accumulation-mode) with both channels prepared by spray deposition method. Overall, the results indicate that the spray-deposition technique provides a convenient route to prepare high performing OECT channels and exhibits great prospects in various ubiquitous electronics and biointegrated organic electronics, such as flexible, conformal biological sensors and foldable wearable integrated circuits.

RESULTS AND DISCUSSION

Figure 1a presents the schematic illustration of the spray deposition process using a commercially available air-brush unit. We fabricated OECTs by spraying a PEDOT:PSS solution onto substrates with pre-patterned gold source-drain electrodes. The spray-coating distance was 10 cm from the spray nozzle to the substrate with a differential pressure of 1.5 bar and performed under ambient conditions. Using this spray-deposition process and a stencil mask, well-defined channels are prepared on top of diverse substrates (see Figure 1b and Figure S1 of Supporting Information). Here, we included an ionic liquid additive in the PEDOT:PSS system to create better electronic and ionic transport in OECTs. In our previous work, we found that counter-ion exchange occurred between PEDOT:PSS and 1-ethyl-3-methylimidazolium tricyanomethanide, [EMIM][TCM] and gave rise to molecular rearrangement, forming a more closely packed order of PEDOT units and fibrillar morphology to facilitate a better pathway for hole transport and enhanced ion penetration.[20] However, the prepared PEDOT:PSS/[EMIM] [TCM] solution was found to be viscous due to the strong molecular interactions and therefore not suitable for spray-printing process. For spray-printing process, the ink has to spread and adhere easily over the surface of substrate. In this work, the OECT performance were obtained from the optimized concentration of a water-soluble ionic liquid, namely, 1-ethyl-3-methylimidazolium chloride, ([EMIM][Cl], 1.1 wt.%) in the PEDOT:PSS solution. The weaker counter-ion exchange & molecular interactions in PEDOT:PSS as compared to [EMIM][TCM] allows better ink formulation and processability. The corresponding molecular interactions was further verified by Grazing-Incidence Wide-Angle X-ray Scattering (GIWAXS); Figure S2. There exist two scattering broad peaks at q = 1.28 $Å^{-1}$ (real space distance d = 4.91 Å, the lattice spacing (d) was obtained from Bragg's law.) and q = 1.78 $Å^{-1}$ (d = 3.53 Å) for PSS side groups and π-π stacking of PEDOT in the pristine film, respectively, in good agreement with previous works.[19] Meanwhile, for PEDOT:PSS/[EMIM][Cl] films, the PSS side group and π-π

stacking of PEDOT is reduced slightly to 1.34 $Å^{-1}$ (4.69 Å) and 1.80 $Å^{-1}$ (3.49 Å) respectively. We also noted similar molecular packing motifs for both spin-coated and spray-coated PEDOT:PSS/[EMIM][Cl] films. A schematic diagram to show the internal structure of ionic-liquid doped PEDOT:PSS is presented in Figure 1c.

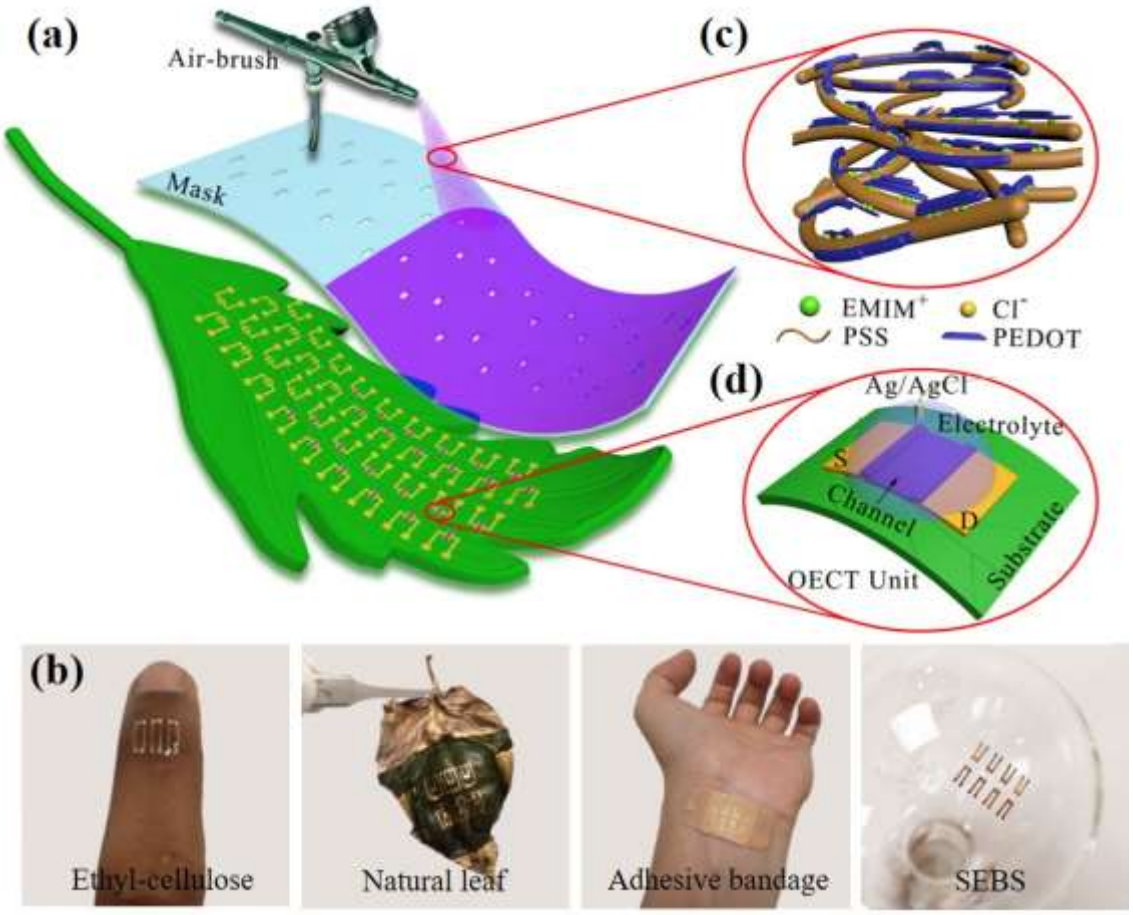

Figure 1. (a) Schematic illustration of the fabrication process using spray-deposition for organic electrochemical transistors. (b) Optical photograph of spray-deposited channel on a variety of substrates including ethyl-cellulose, natural leaf, adhesive bandage, and SEBS elastomer based substrates. (c) A schematic diagram to show the internal structure & molecular packing of spray deposited PEDOT:PSS/[EMIM][Cl] composite. (d) The illustration of a representatively OECT configuration with patterned channel on a supporting leaf substrate.

To complete the device fabrication, a water-based electrolyte (0.1 M NaCl solution) is deposited on top of the spray-deposited PEDOT:PSS/[EMIM][Cl] channel and a non-polarizable Ag/AgCl pellet (1 mm^2) is used as the gate electrode (Figure 1d). The reversible

ionic exchange between the active channel and salt electrolyte is modulated through the application of a gate voltage (V_G). Figure 2a-c first show the OECT electrical performances with a spray-deposited active channel PEDOT:PSS/[EMIM][Cl] on conventional rigid silicon substrate. The PEDOT:PSS/[EMIM][Cl] active channel has a thickness (d) of ~ 400 nm with a width (W) and length (L) of 1000 µm and 250 µm respectively. The output and transfer characteristics of the spray-deposited OECT are presented in Figure 2a-b. The OECT is conducting at zero gate bias owing to the highly doped $PEDOT^+$ state. Consequently, the OECT is switched off around V_G = 0.6 V, exhibiting a depletion mode of operation. A desirable on/off ratio of ~10^3 (drain voltage (V_D) = -0.5 V) can be achieved, owing to the simultaneous enhancement of electronic and ionic transport, as detailed in our previous report.[20] Furthermore, this device shows a high peak transconductance ($g_m = \partial I_D/\partial V_G$) of 12.9 mS at V_G = -0.14 V with V_D = -0.6 V. It is also found that the maximum transconductance, g_m, is closely linked to the applied drain voltage (See Figure 2c). As V_D is lowered, the g_m is decreased. The measured peak g_m, is found to be proportional to the channel geometry ($W*d/L$) with a slope of 4.91 ± 0.30 mS/µm (See Figure S3), in good agreement with the conventional spin-coated devices.[21] When normalized to the channel geometry, the peak g_m is 7.3 mS μm^{-1}, which is also comparable to our spin-cast devices (Figure S4) and other reports (Table S1).[23,32,33]

Good operating stability in aqueous electrolyte media is another paramount requirement when using OECTs as a sensing device in bioelectronics. In this context, a continuous voltage pulse switching, and long-term aging test were carried out to check the stability of the devices. For the continuous pulse measurement, the drain current (I_D) was monitored under a periodical variation of gate bias between -0.4 V and 0.6 V with a pulse width of 0.5 s (V_D = -0.5 V). As shown in Figure 2d, the spray deposited OECT device exhibits a great electrical stability upon successive gate voltage pulses for 4000 cycles. The drain current is maintained >

96% even after 4000 cycles of pulse measurements, indicating minimum degradation processes. This is consistent with previous observations of the ionic-liquid assisted PEDOT:PSS channel exhibiting a highly reversible ion doping/de-doping process in OECT operation.[20] Additionally, the OECT device showed no significant changes in the drain current and maximum transconductance peak, after long-term storage under ambient conditions at room temperature for 6 months without encapsulation (See Figure 2e). All of these results prove that the spray-deposition method can be used to fabricate high-performance OECTs with excellent stability.

It is also useful to benchmark the device performance by using the product of carrier mobility (μ) and volumetric capacitance (C*).[34] The μC^* is extracted from equation $g_m = \frac{\partial I_D}{\partial V_G} = \frac{wd}{L}\,\mu\, C^*(V_T - V_G)$ in the saturation region, where W, L and d are the channel width, length and thickness respectively.[23] The μC^* figure of merit of the spray-coated device is determined to be 84 ± 17 F cm^{-1} V^{-1} s^{-1}. Electrochemical impedance spectroscopy measurements were also carried out to determine the volumetric capacitance independently, exhibiting a C^* of 37.3 ± 3.1 F cm^{-3} (See Figure S5). Based on the μC^* figure of merit from OECT measurements and C^* from impedance data, the corresponding channel mobility is calculated to be 2.26 ± 0.45 cm^2 V^{-1}s^{-1}, comparable to state-of-the-art PEDOT:PSS OECTs.[23]

The transient response (τ) of the drain current was measured by applying a 0.6 V gate pulse with a pulse width of 10 ms (V_D = -0.5 V), and the response time was determined by fitting the drain current with a single exponential decay function.[25] τ is proportional to R_S*C_{CH}, where R_S is the electrolyte resistance and C_{CH} is the channel capacitance. C_{CH} scales with film volume and R_S scales as $R_S \propto 1/\sqrt{WL}$.[21,35] Thus, by putting together the scaling laws for C_{CH} and R_S, $\tau \propto d\sqrt{WL}$.[21] A faster response can therefore be attained by making the channel thinner and smaller channel geometry. As shown in Figure S6a, the response time scales with the channel thickness and geometry for our spray-coated OECT. It was observed that the rise

time of the spray-deposited channel (W/L = 1000 μm/100 μm, d = 101 nm) can go as low as 179 μs, which is comparable with that of other reports (see Figure S6b and Table S2 for the comparison).[23,32,33] Note that the drain current can be completely switched-off even for thick channels, thus indicating good ion penetration and transport in all spray-coated channels, irrespective of channel geometry (See Figure S7).

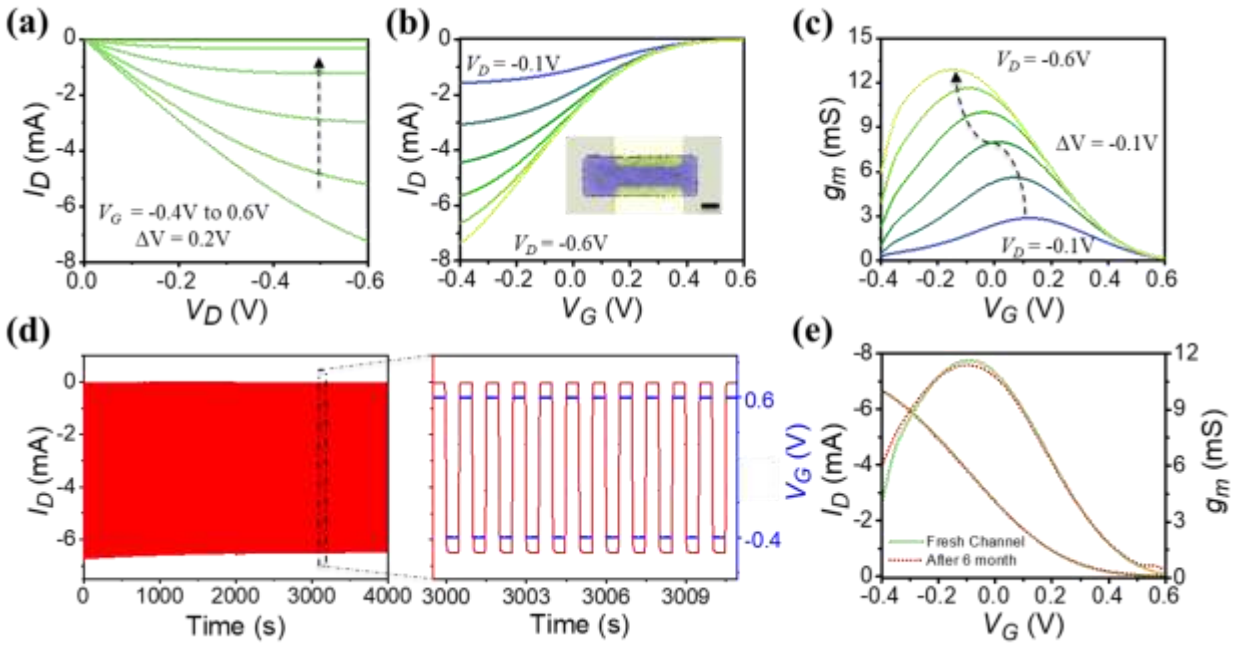

Figure 2. Electrical performance of OECTs. (a) Output characteristics of a representative spray-coated PEDOT:PSS/[EMIM][Cl] based OECT on a silicon substrate. (b) Transfer characteristics of the device under different drain voltages varying from V_D = -0.1 V (bottom curve) to V_D = -0.6 V (top curve) with a step of ΔV = -0.1 V. The inset shows the optical image of the spray-deposited patterned channel, the scale bar is 200 μm, and (c) the associated transconductances at different drain voltages. (d) Pulse measurements (V_G varied from -0.4 V to 0.6 V, pulse length = 0.5 s, V_D = -0.5 V) with over 4000 cycles of continuous operation in 0.1 M NaCl electrolyte. (e) Stability study. Transfer curves of the channel before and after long-term storage in air at room temperature for 6 months, at V_D = -0.5 V.

For a deeper insight into the doping mechanism, the change in the optical absorption spectra of the PEDOT:PSS/[EMIM][Cl] film immersed in the electrolyte under biasing was monitored. Figure 3a shows the absorption spectra under voltage biasing varying from -0.4 V to 1 V in 0.1 M NaCl electrolyte. The initial UV-Vis spectra of PEDOT:PSS/[EMIM][Cl], at zeo bias, has two absorption bands corresponding to a π-π transition located around 650 nm, and a broad absorption band resulting from the polar PEDOT around 970 nm.[20,36] As shown,

the absorption corresponding to the π-π transition is gradually enhanced when increasing the bias from -0.4 V to 1V, indicating an effective de-doping process. This is because the cations (Na^+) injected from the electrolyte into the PEDOT:PSS/[EMIM][Cl] film reduce the highly conducting PEDOT from its bipolaron $PEDOT^{2+}$ state & polaron $PEDOT^+$ state to the neutral semiconducting $PEDOT^0$ state, consistent with previous reports.[36–38] To further investigate the kinetics of de-doping process in the spray-deposited films, bias-dependent absorption at 650 nm and 970 nm was monitored. As shown in Figure 3b, when the voltage bias is increased, the absorption at 650 nm is gently enhanced while the spectral hump around 970 nm derived from the PEDOT polaron is slightly enhanced at a low bias and drops gradually at higher voltage bias due to the existence of the bipolaronic $PEDOT^{2+}$ state. Finally, the bipolaron and polaron absorptions almost disappear at a bias of V_{in} = 1 V. These absorption kinetics results validate the dynamics of de-doping process for PEDOT:PSS, and are consistent with previous works.[20,36]

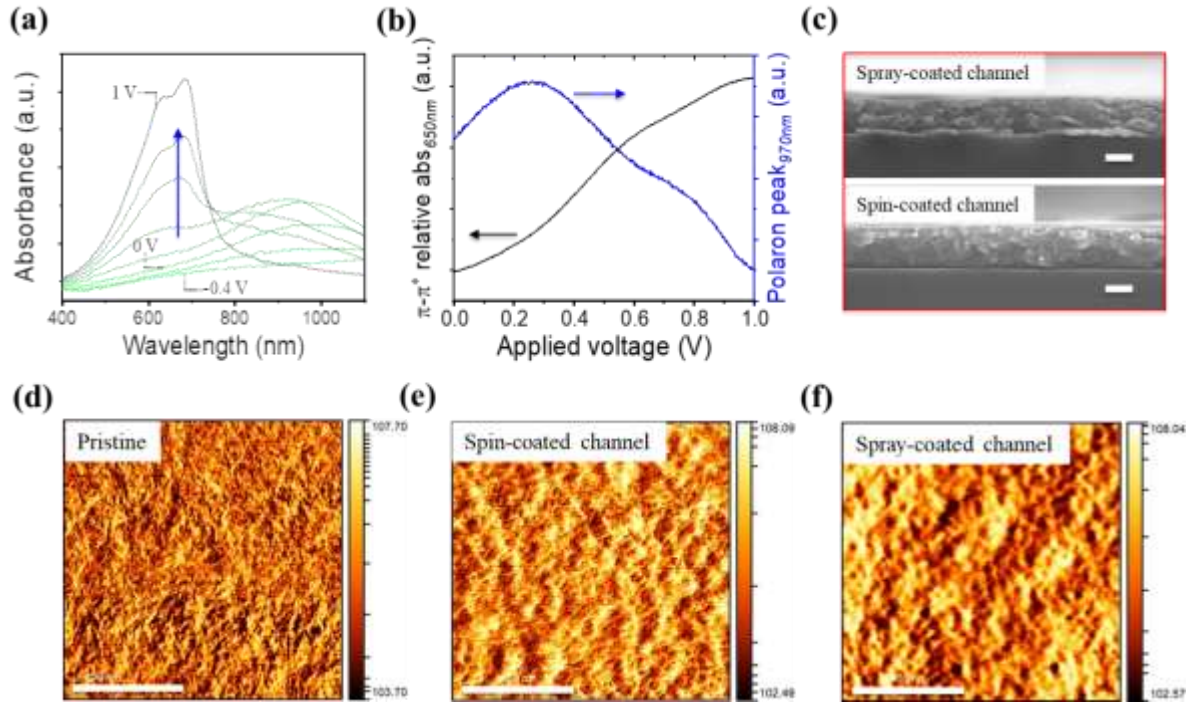

Figure 3. (a) UV-Vis spectra of spray-deposited PEDOT:PSS/[EMIM][Cl] films on ITO coated glass under varying voltage bias (Ag/AgCl pellet) in 0.1 M NaCl electrolyte. The bias voltage varies from -0.4 V to 1 V with a step of ΔV = 0.2 V. (b) Evolution of the relative intensity of π-π* (at 650 nm,

black curve) and polaron (at 970 nm, blue curve) absorption of the spray-deposited PEDOT:PSS film in 0.1 M NaCl electrolyte. (c) Cross-section SEM images of the spray-deposited and spin-coated channels, the scale bar is 200 nm. Atomic force microscopy phase images of the (d) pristine PEDOT:PSS film, (e) spin-coated and (f) spray-deposited PEDOT:PSS/[EMIM][Cl] films, the scale bar is 400 nm.

To explain the device results derived from the spray-deposited channels, we next investigated the 3D cross section morphology and the surface morphology of the spray-deposited PEDOT:PSS and make a comparison with corresponding spin-coated film. The cross-sectional SEM images (see Figure 3c) reveal that the spin and spray deposited films are comparably thick (~ 300 nm), and present similar features and close packed appearance, consistent with the GIWAXS data as discussed earlier and therefore similar device performance (see Figure S4). Further, the atomic force microscopy (AFM) phase images reveal similar PEDOT domains formation (Figure 3d-f) even though the overall surface roughness values of the spin (1.66 nm), and the spray (2.15 nm) deposited films are slightly different. We also observed a clearly enlarged PEDOT-rich domains for PEDOT:PSS/[EMIM][Cl] films compared to pristine PEDOT:PSS.

Many applications for wearable flexible bioelectronics such as sensor skins and implantable devices will require versatile substrates with different textures and form factors. The spray-deposition process is general and applicable to all possible substrate materials. To demonstrate the general applicability of the spray-deposited method for OECTs fabrication, we also investigated the electrical performance and stability of the spray-deposited PEDOT:PSS/[EMIM][Cl]-based channels on a number of substrate materials, including biodegradable flexible substrates based on ethyl-cellulose and natural leaf as well as wearable deformable or elastic substrates based on commercial adhesive bandages and polystyrene-block-poly(ethylene-ran-butylene)-block-polystyrene (SEBS) elastomer (Figure 4). The ethyl-cellulose and SEBS substrates are very thin, around 5.2 μm, and 28 μm of thickness respectively. Figure 4(a), (c), (e) and (g) show the optical images of the sprayed-deposited

channel (~ 400 nm thick) on the various substrates. The spray-deposition method allows fine patterning of the active channel with different channel length varying from 100 μm to 250 μm on these substrates. More importantly, it is found that all of these spray-deposited channels exhibit good device performance with high transconductance of 8.8 mS, 6.8 mS, 5.3 mS, and 6.7 mS on ethyl-cellulose-, leaf-, adhesive bandage-, and SEBS-based substrates respectively. The associated drain current response time (switch off) are 1.93 ms, 0.93 ms, 0.74 ms, and 0.72 ms (see Figure S8). Though the surface textures of these substrates are varied, the devices still exhibit high electrical stability even after 200 cycles of pulsed measurements (V_G varied from -0.4 V to 0.6 V, pulse length = 0.5 s, V_D = -0.5 V), as shown in Figure S9 of the supporting information. This result further proves that the spray-deposition technique provides a facile method to prepare high performance OECTs for a wide variety of applications.

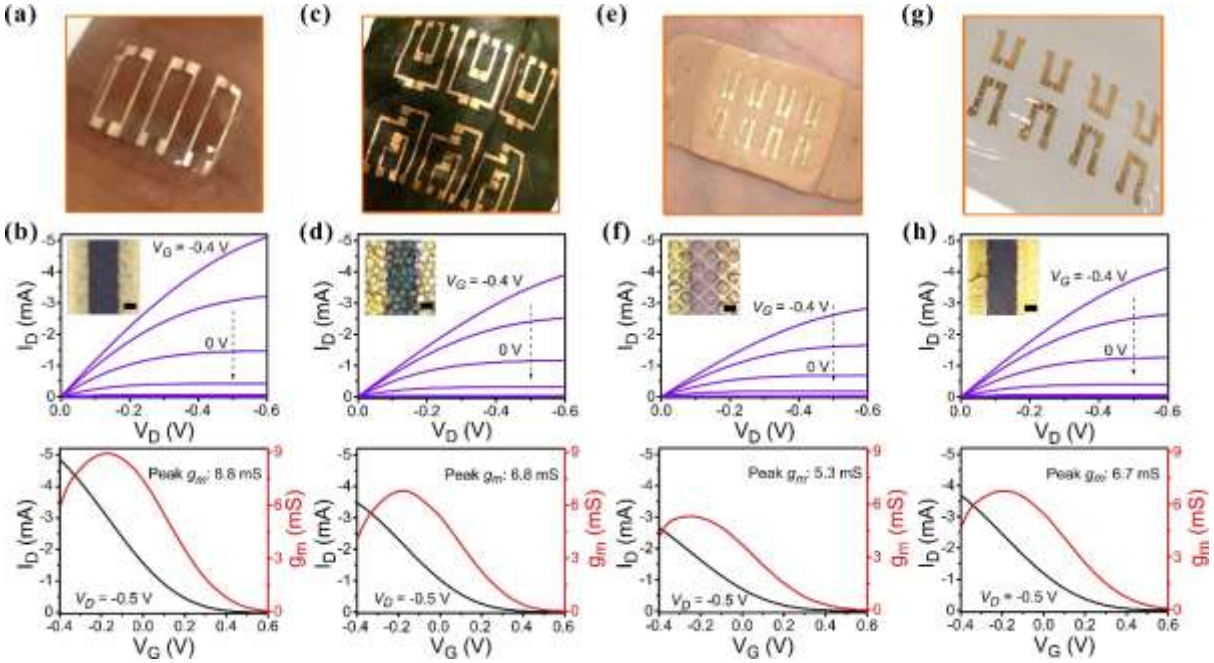

Figure 4. Electrical performance of OECTs on different substrates with different surface textures. Optical images of the OECTs on (a) biodegradable ethyl-cellulose-, (c) natural leaf, (e) commercial adhesive bandage, and (g) SEBS elastomer-based substrates, (b-h) the corresponding output, transfer and transconductance characteristics of the OECTs. For the output characteristics, V_G = -0.4 V to 0.6 V (top to bottom) with a step of 0.2 V. For the transfer characteristics, V_D = -0.5 V and the associated transconductance is also plotted. The

inset is the optical microscopy image of spray-deposited channels on the corresponding substrates W/L = 1000 μm/250 μm, thickness d = ~400 nm).

To further explore the applicability of the spray-deposition process to other active materials, we also look at spray-deposition of glycolated thiophene (g2T-T) polymer. g2T-T is the one of state-of-the-art p-type semiconducting polymers, which has been reported to work as an efficient and highly stable electroactive material for OECTs.[39] Figure 5(a-c) presents the output characteristic and transfer curve of a 115 nm thick g2T-T OECT with a channel width and length of 1000 μm and 100 μm respectively. Upon application of a negative gate bias, anions from the electrolyte inject in the active layer, giving rise to an electrochemical doping of g2T-T, which is accompanied with the increase of the drain-current. As a result, the channel was switched on with a peak drain current of 2.4 mA (V_G = -0.6 V), the corresponding peak g_m reaches 7.8 mS at V_D = -0.4 V. In comparison with reported spin-coated device, the normalized peak transconductance (by channel dimension Wd/L) is similar ($g_{m,\ max}$ = 7.9 mS, W/L = 100 μm/10 μm, thickness d = 103 nm).[39] Furthermore, this spray-deposition method also makes it possible to fabricate a fully spray-deposited inverter. As known, inverters are the most basic elements in a circuit and are commonly used to construct logic gates or amplifiers for biological components. The inset in Figure 5c represents a simple logic circuit of the inverter, which consists of two p-type OECTs (g2T-T and PEDOT:PSS). Note that both of the OECT channels were prepared by spray-deposition method. The accumulation-mode g2T-T-based OECT was connected to the depletion-mode PEDOT:PSS-based OECT to form the inverter. Also note that the thickness of the PEDOT:PSS channel was optimized of ~50 nm to match the g2T-T channel. The resulting inverter characteristics are given in Figure 5c. When the supply voltage (V_{DD}) is set to 0.8 V and the input voltage (V_{in}) is swept from 0 to 0.5 V, a relatively high gain ($\partial V_{out}/\partial V_{in}$) value of 18 is obtained.

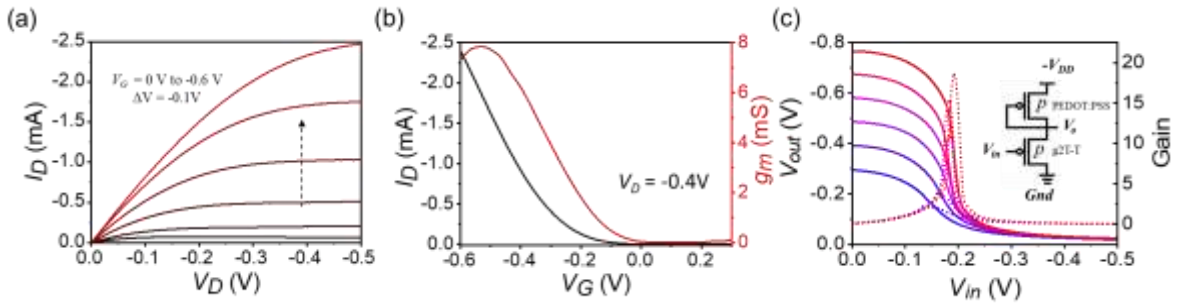

Figure 5. Electrical performance of spray-deposited g2T-T-based OECTs. (a) Representative output characteristics of the spray-deposited g2T-T OECT. (b) Transfer curve and the associated transconductance. The transfer curve was measured at V_D = -0.4 V. The channel W/L = 1000 μm /100 μm, d = 115 nm. This device was measured in 0.1 M NaCl. (c) Input-output characteristics of an inverter consisting of two p-type OECTs: one employing a PEDOT:PSS and one a g2T-T active channel material, and the associated voltage gains ($\partial V_{out}/\partial V_{in}$). Inset is the schematic of the inverter.

CONCLUSIONS

In conclusion, we successfully demonstrated a facile spray-deposition technique to fabricate PEDOT:PSS-based OECTs with high transconductance and excellent stability. Our channel patterning approach does not involve organic solvents or complex lithography techniques and we are able to obtain defined polymer channels directly on various flexible substrates. Notably, the optimized spray deposited OECT yields a high normalized peak transconductance of 14.5 mS $V^{-1}\mu m^{-1}$, while the device exhibits excellent stability during pulsed gate measurements with over 4000 cycles of continuous operation in 0.1 M NaCl electrolyte. A long-term stability over six months storage under ambient conditions was also observed. Furthermore, we have explored various nonplanar flexible substrates for spray-deposited PEDOT:PSS based OECTs which possess high electrical performance with transconductance values ranging from 3.7 – 7.4 mS at V_G = 0 V and on/off ratio of ~5×10^2. Additionally, we presented an inverter based entirely on OECTs with a high gain of ~18 by combining a PEDOT:PSS OECT (depletion-mode) and a g2T-T OECT (accumulation-mode) with both channels prepared by the spray deposition method. We believe that the present study and findings will contribute to the translation of OECTs into real-world applications.

METHODS

Materials and Chemicals. Poly(3,4-ethylenedioxythiophene):poly(styrenesulfonate) (PEDOT:PSS, Clevios PH1000) were obtained from Heraeus. 1-Ethyl-3-methylimidazolium chloride ([EMIM][Cl]), (3-glycidyloxypropyl)trimethoxysilane (GOPS), ethyl-cellulose, sodium chloride (NaCl) and all the processing solvents including acetone, ethanol and toluene were purchased from Sigma-Aldrich and used as received. Styrene ethylene butylene styrene (SEBS) was obtained from AK Elastomer. The adhesive bandage is commercially available and used as received. The p-Si^{++}/SiO_2 wafers were purchased from Addison Engineering, Inc, while the ITO substrates were purchased from Xin Yan Technology Ltd.

Substrates preparation. All the p-Si^{++}/SiO_2 (200 nm) substrates were pre-cleaned successively in a sonicated bath using soap water, distilled water, acetone and ethanol for 10 min each. The ethyl-cellulose substrates were prepared from an ethanol solution (10 mg/ml) spin-casted on glass slide, and annealing at 60 °C for 10 min. To prepare the SEBS elastomer substrates, the SEBS was dissolved in toluene (150 mg/ml) first. The prepared SEBS solution were spin-coated on a glass slide and dried at room temperature to form a uniform substrate. Meanwhile, the natural leaf was collected from a common plant, and was used without any further treatment.

OECT Fabrication. In OECTs fabrication, all the substrates including p-Si^{++}/SiO_2 (200 nm) wafer, leaf, bandage, SEBS and ethyl-cellulose were pre-deposited with source and drain electrodes (10 nm Ni/ 90 nm Au) using thermal evaporation process. To prepare a well patterned active channel for OECT, a filtered (using 0.45 μm hydrophilic PVDF filters) PEDOT:PSS aqueous solution (1 ml) was mixed with [EMIM][Cl] (0.075 mmol, 0.05 M in DI water) and GOPS (5 μl), vigorously stirred for 1h at room temperature. After that, the mixed solution was spray-deposited on the corresponding substrates (p-Si^{++}/SiO_2 wafer, ethyl-cellulose, leaf, bandage and SEBS) through a shadow mask, using a commercial air-

brush (Model ASG-Ko82). For the spray setup, a commercial airbrush (Model ASG-K082) with a nozzle diameter of 0.3 mm was connected to a nitrogen gas line with air pressure valve. To have a highly reproduceable and consistent of the spray-deposited PEDOT:PSS channel, the spray-deposition procedure was optimized as follow: the nozzle-to-substrate distance was around 10 cm; the gas flow pressure is fixed at 1.5 bar to produce uniform PEDOT:PSS fog over the substrates; the relative humidity is around 65%; the used substrate temperature for this spray-deposition procedure is set at 100°C (measured by infrared thermometer) to dry the spray-deposited PEDOT:PSS channel. The spray-time was controlled to obtain different channel thickness. After that, the substrate was maintained on the hotplate for around 15 min to ensure fully dry the spray-deposited channels. To fabricate the spray-deposited g2T-T OECT, 1 mg/ml g2T-T solution was prepared by dissolving the polymer in chloroform. The spray deposition process was carried out similar to the PEDOT:PSS OECTs. However, the whole deposition process was completed at room temperature without heating the substrate to enable the g2T-T solution spread and merge together and form a uniform channel, and the g2T-T channel was used as prepared without further annealing.

Materials Characterization. FE-SEM (JOEL JSM-7600F) was performed to check the internal structure of the active channels. Both spray-deposited and spin-coated channels were measured after normal OECT characterizations. The measured channels were rinsed with deionized water and dried at 140 °C for 10 min before FE-SEM characterization. UV-vis-NIR spectrophotometer (SHIMADZU, UV-3600) was used to record the absorption spectra of the PEDOT:PSS-based films. To check the absorption spectrums variation of the PEDOT:PSS-based film under biasing, an experimental setup was built as reported in our previous literature.[20] In brief, the PEDOT:PSS-based films were spray-deposited on ITO glass substrates with a patterned area of 10 mm × 5 mm (thickness d = ~ 200 nm) through a shadow mask, and annealed at 140 °C for 20 min. The prepared films were rinsed with

deionized water before measurement, and then immersed into a cuvette with 0.1 M NaCl solution. An external bias was applied on the spray-deposited film between ITO glass and an Ag/AgCl pellet (1 mm^2) using a Keysight precision source/measure unit (B2912A). All the films thickness were measured using a surface profiler (Alpha-step, KLA-Tencor). Electrical impedance spectroscopy (Autolab PGSTAT 128N) was carried out to extract the film volumetric capacitance using a three-terminal configuration. A PEDOT:PSS film patterned on top of Ni/Au (10/90) electrodes as working electrode, and Ag/AgCl wire and Pt mesh as reference and counter electrode, respectively. This measurement was performed over a range of 10 MHz to 1 Hz with an AC amplitude of 10 mV sine wave in 0.1 M NaCl aqueous electrolyte. Atomic force microscope (AFM) (Cypher S) was carried out to check the film morphology in tapping mode. Grazing incidence wide angle X-ray diffraction (GIWAXS; Nanoinxider Xenocs) was employed to study the molecular packing of the pristine PEDOT:PSS and PEDOT:PSS/[EMIM][Cl] films.

OECT Characterization. All the electrical characteristics of OECTs were conducted using Keysight precision source/measure unit (B2900A Series) under ambient at room temperature. For the OECTs characteristic, an Ag/AgCl pellet was employed as a gate electrode and immersed in the 0.1 M NaCl electrolyte.

Supporting Information

The Supporting Information is available free of charge on the ACS Publications website or from the author. Schematic illustration of spray-deposition process; grazing-Incidence wide-angle x-ray scattering (GIWAXS) of the spin-coated pristine PEDOT:PSS film, spin-coated and spray deposited PEDOT:PSS/[EMIM][Cl] film; peak transconductance of spray deposited and spin coated OECTs as a function of active layer dimensionality; transfer curves and the associated transconductance of spray-deposited and spin-coated channel with same channel geometry dimensions, comparison of the transconductance of spin-coated and spray-deposited PEDOT:PSS-based OECTs; impedance spectra of the spray-deposited PEDOT:PSS film in 0.1 M NaCl solution, transient responses of the spray-coated channels and as a function of $d\sqrt{WL}$; comparison of transient responses of PEDOT:PSS OECTs fabricated by spin-coat and spray-deposit method; transient response of the corresponding drain current on

a various of substrates including biodegradable ethyl-cellulose, natural leaf, commercial adhesive bandage, and SEBS elastomer; stability study of OECTs on various substrates through pulse measurements with over 200 cycles of continuous operation in 0.1 M NaCl electrolyte.

Acknowledgements

W.L. Leong would like to acknowledge funding support from her NTU start-up grant (M4081866), Ministry of Education (MOE) under AcRF Tier 2 grant (2018-T2-1-075) and A*STAR AME Young Individual Research Grant (Project Number A1784c019). The authors would like to thank Prof. Nripan Mathews for useful discussions.

Received: ((will be filled in by the editorial staff))

Revised: ((will be filled in by the editorial staff))

Published online: ((will be filled in by the editorial staff))

References

(1) Sessolo, M.; Khodagholy, D.; Rivnay, J.; Maddalena, F.; Gleyzes, M.; Steidl, E.; Buisson, B.; Malliaras, G. G. Easy-to-Fabricate Conducting Polymer Microelectrode Arrays. *Adv. Mater.* **2013**, *25*, 2135–2139.

(2) Rivnay, J.; Inal, S.; Salleo, A.; Owens, R. M.; Berggren, M.; Malliaras, G. G. Organic Electrochemical Transistors. *Nat. Rev. Mater.* **2018**, *3*, 17086.

(3) Lee, W.; Kobayashi, S.; Nagase, M.; Jimbo, Y.; Saito, I.; Inoue, Y.; Yambe, T.; Sekino, M.; Malliaras, G. G.; Yokota, T.; Tanaka, M. Nonthrombogenic, Stretchable, Active Multielectrode Array for Electroanatomical Mapping. *Sci. Adv.* **2018**, *4* , eaau2426.

(4) Chen, L.; Fu, Y.; Wang, N.; Yang, A.; Li, Y.; Wu, J.; Ju, H.; Yan, F. Organic Electrochemical Transistors for the Detection of Cell Surface Glycans. *ACS Appl.*

Mater. Interfaces **2018**, *10*, 18470–18477.

(5) Qing, X.; Wang, Y.; Zhang, Y.; Ding, X.; Zhong, W.; Wang, D.; Wang, W.; Liu, Q.; Liu, K.; Li, M.; Lu, Z. Wearable Fiber-Based Organic Electrochemical Transistors as a Platform for Highly Sensitive Dopamine Monitoring. *ACS Appl. Mater. Interfaces* **2019**, *11*, 13105–13113.

(6) Tang, H.; Yan, F.; Lin, P.; Xu, J.; Chan, H. L. W. Highly Sensitive Glucose Biosensors Based on Organic Electrochemical Transistors Using Platinum Gate Electrodes Modified with Enzyme and Nanomaterials. *Adv. Funct. Mater.* **2011**, *21*, 2264–2272.

(7) Tao, W.; Lin, P.; Hu, J.; Ke, S.; Song, J.; Zeng, X. A Sensitive DNA Sensor Based on an Organic Electrochemical Transistor Using a Peptide Nucleic Acid-Modified Nanoporous Gold Gate Electrode. *RSC Adv.* **2017**, *7*, 52118–52124.

(8) Lin, P.; Luo, X.; Hsing, I. M.; Yan, F. Organic Electrochemical Transistors Integrated in Flexible Microfluidic Systems and Used for Label-Free DNA Sensing. *Adv. Mater.* **2011**, *23*, 4035–4040.

(9) Coppedè, N.; Tarabella, G.; Villani, M.; Calestani, D.; Iannotta, S.; Zappettini, A. Human Stress Monitoring through an Organic Cotton-Fiber Biosensor. *J. Mater. Chem. B* **2014**, *2*, 5620–5626.

(10) Ludwig, K. A.; Langhals, N. B.; Joseph, M. D.; Richardson-Burns, S. M.; Hendricks, J. L.; Kipke, D. R. Poly(3,4-Ethylenedioxythiophene) (PEDOT) Polymer Coatings Facilitate Smaller Neural Recording Electrodes. *J. Neural Eng.* **2011**, *8*, 014001.

(11) Green, R. A.; Lovell, N. H.; Wallace, G. G.; Poole-Warren, L. A. Conducting Polymers for Neural Interfaces: Challenges in Developing an Effective Long-Term Implant. *Biomaterials* **2008**, *29*, 3393–3399.

(12) Basiricò, L.; Cosseddu, P.; Scidà, A.; Fraboni, B.; Malliaras, G. G.; Bonfiglio, A. Electrical Characteristics of Ink-Jet Printed, All-Polymer Electrochemical Transistors. *Org. Electron.* **2012**, *13*, 244–248.

(13) Andersson Ersman, P.; Nilsson, D.; Kawahara, J.; Gustafsson, G.; Berggren, M. Fast-Switching All-Printed Organic Electrochemical Transistors. *Org. Electron.* **2013**, *14* , 1276–1280.

(14) Yuen, J. D.; Walper, S. A.; Melde, B. J.; Daniele, M. A.; Stenger, D. A. Electrolyte-Sensing Transistor Decals Enabled by Ultrathin Microbial Nanocellulose. *Sci. Rep.* **2017**, *7*, 40867.

(15) Afonso, M.; Morgado, J.; Alcácer, L. Inkjet Printed Organic Electrochemical Transistors with Highly Conducting Polymer Electrolytes. *J. Appl. Phys.* **2016**, *120*, 165502.

(16) Li, Y.; Wang, N.; Yang, A.; Ling, H.; Yan, F. Biomimicking Stretchable Organic Electrochemical Transistor. *Adv. Electron. Mater.* **2019**, 1900566.

(17) Rivnay, J.; Inal, S.; Collins, B. A.; Sessolo, M.; Stavrinidou, E.; Strakosas, X.; Tassone, C.; Delongchamp, D. M.; Malliaras, G. G. Structural Control of Mixed Ionic and Electronic Transport in Conducting Polymers. *Nat. Commun.* **2016**, *7*, 11287.

(18) Palumbiny, C. M.; Heller, C.; Schaffer, C. J.; Körstgens, V.; Santoro, G.; Roth, S. V.; Müller-Buschbaum, P. Molecular Reorientation and Structural Changes in Cosolvent-Treated Highly Conductive PEDOT:PSS Electrodes for Flexible Indium Tin Oxide-Free Organic Electronics. *J. Phys. Chem. C.* **2014**, *118*, 13598–13606.

(19) Palumbiny, C. M.; Liu, F.; Russell, T. P.; Hexemer, A.; Wang, C.; Müller-Buschbaum, P. The Crystallization of PEDOT:PSS Polymeric Electrodes Probed In Situ during

Printing. *Adv. Mater.* **2015**, *27*, 3391–3397.

(20) Wu, X.; Surendran, A.; Ko, J.; Filonik, O.; Herzig, E. M.; Müller-Buschbaum, P.; Leong, W. L. Ionic-Liquid Doping Enables High Transconductance, Fast Response Time, and High Ion Sensitivity in Organic Electrochemical Transistors. *Adv. Mater.* **2019**, *31*, 1805544.

(21) Friedlein, J. T.; McLeod, R. R.; Rivnay, J. Device Physics of Organic Electrochemical Transistors. *Org. Electron.* **2018**, *63*, 398–414.

(22) Đerek, V.; Jakešová, M.; Berggren, M.; Simon, D. T.; Głowacki, E. D. Micropatterning of Organic Electronic Materials Using a Facile Aqueous Photolithographic Process. *AIP Adv.* **2018**, *8*, 105116.

(23) Rivnay, J.; Leleux, P.; Ferro, M.; Sessolo, M.; Williamson, A.; Koutsouras, D. A.; Khodagholy, D.; Ramuz, M.; Strakosas, X.; Owens, R. M,; Benar, C. High-Performance Transistors for Bioelectronics through Tuning of Channel Thickness. *Sci. Adv.* **2015**, *1*, e1400251.

(24) Xia, Y.; Zhang, W.; Ha, M.; Cho, J. H.; Renn, M. J.; Kim, C. H.; Frisbie, C. D. Printed Sub-2 V Gel-Electrolyte-Gated Polymer Transistors and Circuits. *Adv. Funct. Mater.* **2010**, *20*, 587–594.

(25) Sun, H.; Vagin, M.; Wang, S.; Crispin, X.; Forchheimer, R.; Berggren, M.; Fabiano, S. Complementary Logic Circuits Based on High-Performance n-Type Organic Electrochemical Transistors. *Adv. Mater.* **2018**, *30*, 1704916.

(26) Tarabella, G.; Vurro, D.; Lai, S.; D'Angelo, P.; Ascari, L.; Iannotta, S. Aerosol Jet Printing of PEDOT:PSS for Large Area Flexible Electronics. *Flex. Print. Electron.* **2020**, *5*, 014005.

(27) Buffet, A.; Abul Kashem, M. M.; Perlich, J.; Herzog, G.; Schwartzkopf, M.; Gehrke, R.; Roth, S. V. Stripe-Like Pattern Formation in Airbrush-Spray Deposition of Colloidal Polymer Film. *Adv. Eng. Mater.* **2010**, *12*, 1235–1239.

(28) Herzog, G.; Benecke, G.; Buffet, A.; Heidmann, B.; Perlich, J.; Risch, J. F. H.; Santoro, G.; Schwartzkopf, M.; Yu, S.; Wurth, W.; Roth, S. V. In Situ Grazing Incidence Small-Angle X-Ray Scattering Investigation of Polystyrene Nanoparticle Spray Deposition onto Silicon. *Langmuir* **2013**, *29*, 11260–11266.

(29) Al-Hussein, M.; Schindler, M.; Ruderer, M. A.; Perlich, J.; Schwartzkopf, M.; Herzog, G.; Heidmann, B.; Buffet, A.; Roth, S. V.; Müller-Buschbaum, P. In Situ X-Ray Study of the Structural Evolution of Gold Nano-Domains by Spray Deposition on Thin Conductive P3HT Films. *Langmuir* **2013**, *29*, 2490–2497.

(30) Lee, M. Y.; Lee, H. R.; Park, C. H.; Han, S. G.; Oh, J. H. Organic Transistor-Based Chemical Sensors for Wearable Bioelectronics. *Acc. Chem. Res.* **2018**, *51* , 2829–2838.

(31) Ramesh, M.; Boopathi, K. M.; Huang, T.-Y.; Huang, Y.-C.; Tsao, C.-S.; Chu, C.-W. Using an Airbrush Pen for Layer-by-Layer Growth of Continuous Perovskite Thin Films for Hybrid Solar Cells. *ACS Appl. Mater. Interfaces* **2015**, *7*, 2359–2366.

(32) Khodagholy, D.; Rivnay, J.; Sessolo, M.; Gurfinkel, M.; Leleux, P.; Jimison, L. H.; Stavrinidou, E.; Herve, T.; Sanaur, S.; Owens, R. M.; Malliaras, G.G. High Transconductance Organic Electrochemical Transistors. *Nat. Commun.* **2013**, *4*, 2133.

(33) Spyropoulos, G. D.; Gelinas, J. N.; Khodagholy, D. Internal Ion-Gated Organic Electrochemical Transistor: A Building Block for Integrated Bioelectronics. *Sci. Adv.* **2019**, *5*, eaau7378.

(34) Inal, S.; Malliaras, G. G.; Rivnay, J. Benchmarking Organic Mixed Conductors for

Transistors. *Nat. Commun.* **2017**, *8*, 1767.

(35) Koutsouras, D. A.; Gkoupidenis, P.; Stolz, C.; Subramanian, V.; Malliaras, G. G.; Martin, D. C. Impedance Spectroscopy of Spin-Cast and Electrochemically Deposited PEDOT:PSS Films on Microfabricated Electrodes with Various Areas. ChemElectroChem 2017, *4*, 2321–2327.

(36) Ouyang, J.; Xu, Q.; Chu, C.-W.; Yang, Y.; Li, G.; Shinar, J. On the Mechanism of Conductivity Enhancement in Poly(3,4-Ethylenedioxythiophene):Poly(Styrene Sulfonate) Film through Solvent Treatment. *Polymer.* **2004**, *45*, 8443–8450.

(37) Lee, S. H.; Park, H.; Kim, S.; Son, W.; Cheong, I. W.; Kim, J. H. Transparent and Flexible Organic Semiconductor Nanofilms with Enhanced Thermoelectric Efficiency. *J. Mater. Chem. A* **2014**, *2*, 7288–7294.

(38) Park, B. W.; Yang, L.; Johansson, E. M. J.; Vlachopoulos, N.; Chams, A.; Perruchot, C.; Jouini, M.; Boschloo, G.; Hagfeldt, A. Neutral, Polaron, and Bipolaron States in Pedot Prepared by Photoelectrochemical Polymerization and the Effect on Charge Generation Mechanism in the Solid-State Dye-Sensitized Solar Cell. *J. Phys. Chem. C* **2013**, *117*, 22484–22491.

(39) Nielsen, C. B.; Giovannitti, A.; Sbircea, D. T.; Bandiello, E.; Niazi, M. R.; Hanifi, D. A.; Sessolo, M.; Amassian, A.; Malliaras, G. G.; Rivnay, J.; McCulloch, I. Molecular Design of Semiconducting Polymers for High-Performance Organic Electrochemical Transistors. *J. Am. Chem. Soc.* **2016**, *138*, 10252–10259.

Supporting Information

Universal spray-deposition process for scalable, high performance and stable organic electrochemical transistors

*Xihu Wu, Abhijith Surendran, Maximilian Moser, Shuai Chen, Bening Tirta Muhammad, Iuliana Petruta Maria, Iain McCulloch and Wei Lin Leong**

X. Wu, A. Surendran, Dr. S. Chen, B. T. Muhammad, Prof. W. L. Leong
School of Electrical Electronic Engineering
Nanyang Technological University
50 Nanyang Avenue, Singapore 639798, Singapore
E-mail: wlleong@ntu.edu.sg

M. Moser, I.P. Maria, Prof. I. McCulloch
Department of Chemistry,
Imperial College London, London, SW7 2AX, UK

B. T. Muhammad
Interdisciplinary Graduate School, Nanyang Technological University, 50 Nanyang Avenue, Singapore 639798, Singapore

Prof. I. McCulloch
King Abdullah University of Science and Technology (KAUST), Physical Sciences and Engineering Division, KAUST Solar Center (KSC), Thuwal 23955-6900, Saudi Arabia

Figure S1. Schematic illustration of the patterning process using spray-deposition for organic electrochemical transistors. The inset shows an optical image of a representative patterned active channel on Si-substrate, the scale bar is 200 µm.

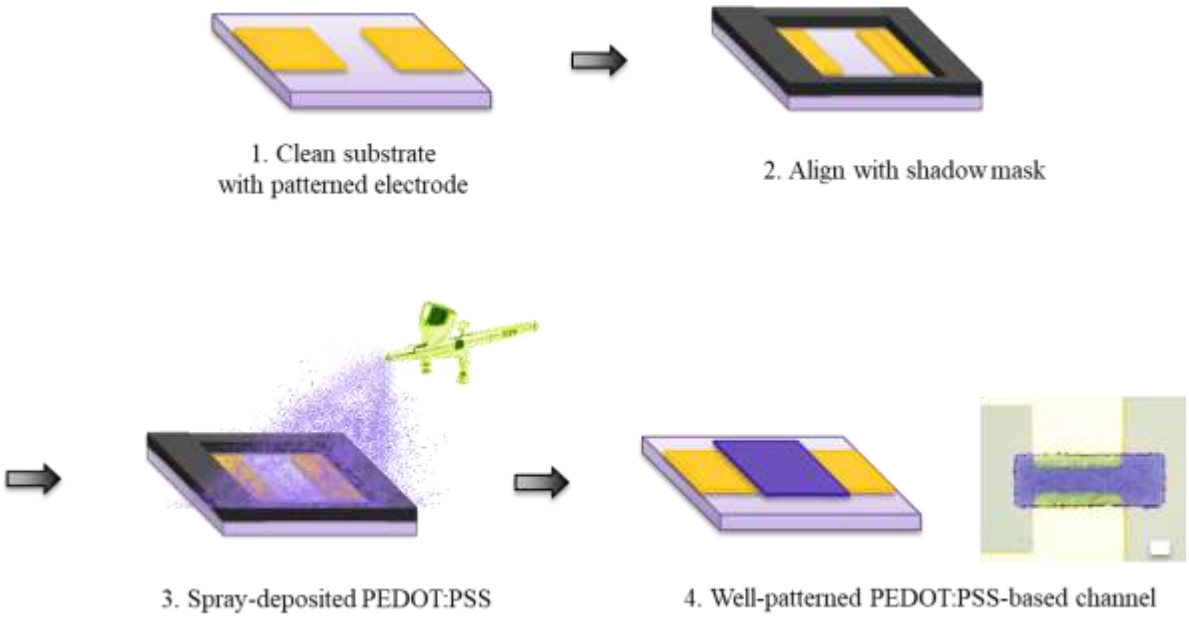

Figure S2. Grazing-Incidence Wide-Angle X-ray Scattering (GIWAXS) of the spin-coated pristine PEDOT:PSS film, spin-coated and spray deposited PEDOT:PSS/[EMIM][Cl] film.

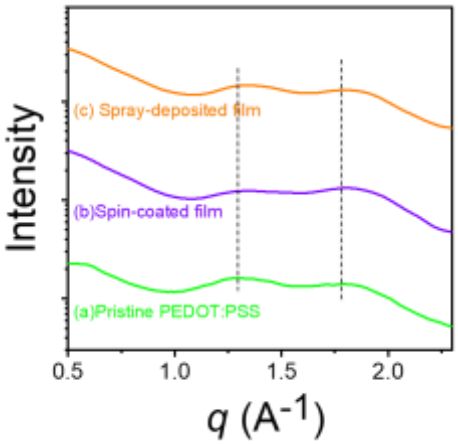

Figure S3. (a) Peak transconductance of spray deposited (solid-black star) and spin coated (open-violet circle) OECTs as a function of active layer dimensionality (*W*d/L*), the peak transconductances were calculated from transfer characteristics under V_D = -0.5 V. The inset red dash-dot curve represents their linear relationship with slope of 4.91 ± 0.30 mS/μm.

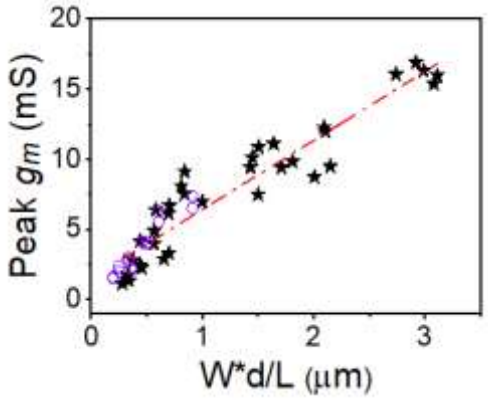

Figure S4. Transfer curves and the associated transconductance of (a) spray-deposited and (b) spin-coated channel with same channel W/L = 1000 /250μm and comparable thickness of ~ 100 nm. The corresponding transconductances were calculated from transfer characteristics under V_D = -0.5 V.

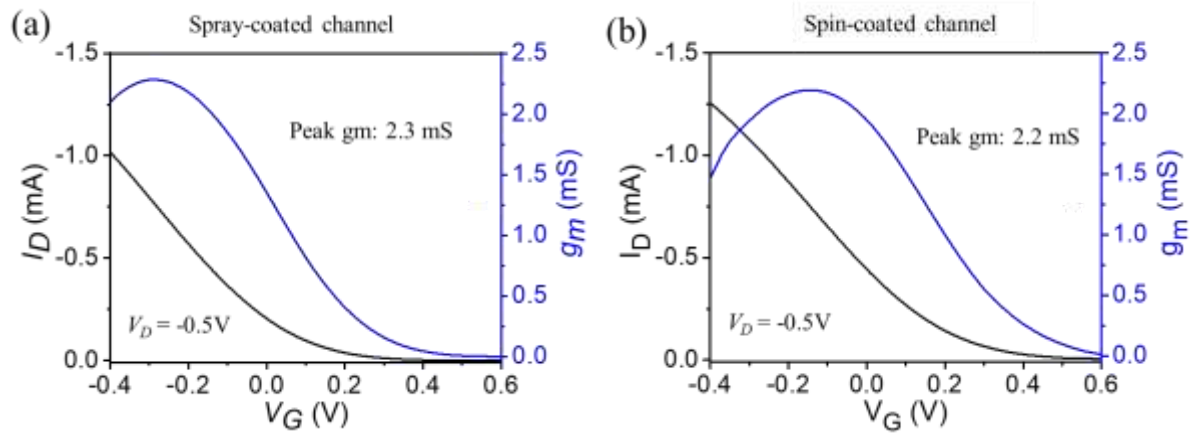

Table S1. Comparison of the transconductance of spin-coated and spray-deposited PEDOT:PSS-based OECTs.

Deposition Process	W/L (μm/ μm)	Thickness (nm)	dW/L (μm)	V_D (V)	Peak g_m (mS)	$g_m/(d \cdot W/L)$ (mS/ μm)	C* (F cm^{-3})	Mobility μ (cm^2 $V^{-1}s^{-1}$)	Reference
Spin coating	10/5	400	0.4	-0.6	2.7	6.5	-	-	[1]
	50/50	500	0.5	-0.5	5.0	10.0	39.3 ± 1.3	1.9 ± 1.3	[2]
	12/30	~200	0.08	-0.6	0.8	10.0	-	-	[3]
Spray coating	**1000/250**	**400**	**1.6**	**-0.5**	**11.6**	**7.3**	**37.3 ± 3.1**	**2.26 ± 0.45**	**This work**

Figure S5. (a) Impedance spectra of the spray-deposited PEDOT:PSS film in 0.1 M NaCl solution, in which the PEDOT:PSS film was deposited on top of Ni/Au electrode and used as the working electrode, with a standard Ag/AgCl wire and Pt mesh as reference electrode and counter electrode, respectively. The impedance data is fit to an equivalent circuit of $R_s(R_p||C)$. (b) The capacitance (C) as a function of the deposited film volume. Inset is the linear fitting of the capacitance and volume, the slope of 37.3 ± 3.1 represents the corresponding volumetric capacitance (C*).

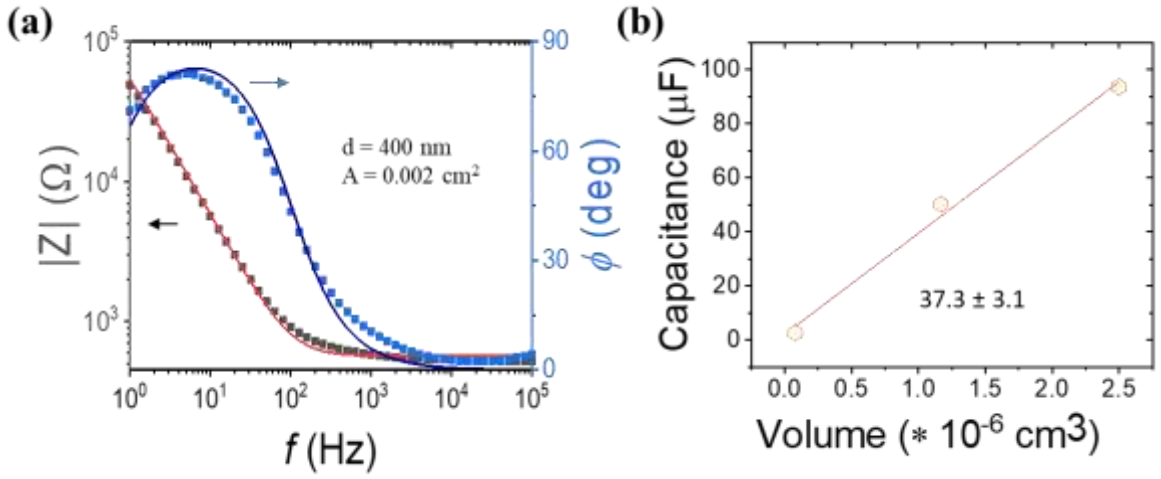

Figure S6. (a) Transient response of the spray-coated channels as a function of $d\sqrt{WL}$. The drain current response time was measured under a square voltage bias of V_G varying from 0 V to 0.6 V. And the rise time was determined by fitting the drain current with a single exponential decay function. (b) The fastest transient responses of the spray deposited OECT (W/L = 1000 μm/100 μm, thickness d = 101 nm).

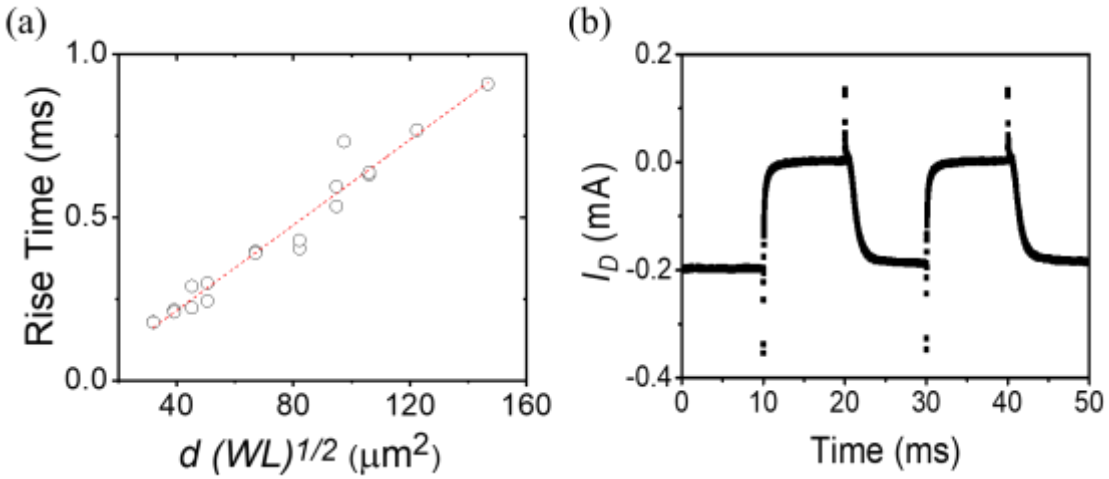

Table S2. Comparison of transient responses of PEDOT:PSS OECTs fabricated by spin-coat and spray-deposit method.

W/L (μm/ μm)	Thickness (nm)	$d\sqrt{WL}$ (μm^2)	Rise time (μs)	Reference
10/10	400	4	102	[1]
50/50	500	25	320	[2]
12/30	~200	3.8	191.2	[3]
1000/100	101	67	179	This work

Figure S7. Transient responses of the spray deposited OECT (W/L = 1000 μm/100 μm, thickness d = 613 nm). The drain current response time was measured under a square voltage bias of V_G varying from 0 V to 0.6 V. And the rise time was determined by fitting the drain current with a single exponential decay function. The red line is an exponential fit to extract the rise time τ = 740 μs.

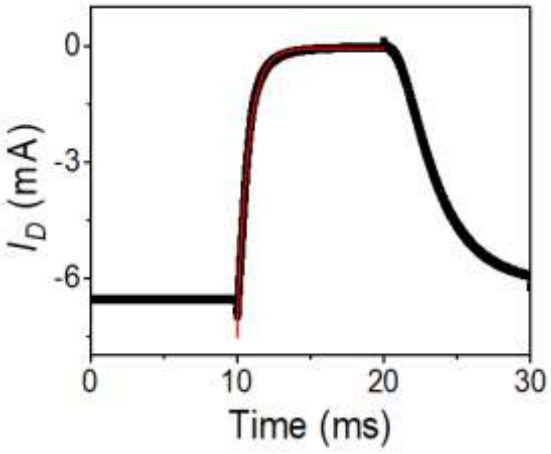

Figure S8. Transient response of the corresponding drain current of OECTs on various substrates including (a) biodegradable ethyl-cellulose and (b) natural leaf, (c) commercial adhesive bandage, and (d) SEBS elastomer. A gate pulse of 50 ms (V_G = 0.6 V) was applied, at V_D = -0.5 V. The red line is an exponential fit to extract the rise time.

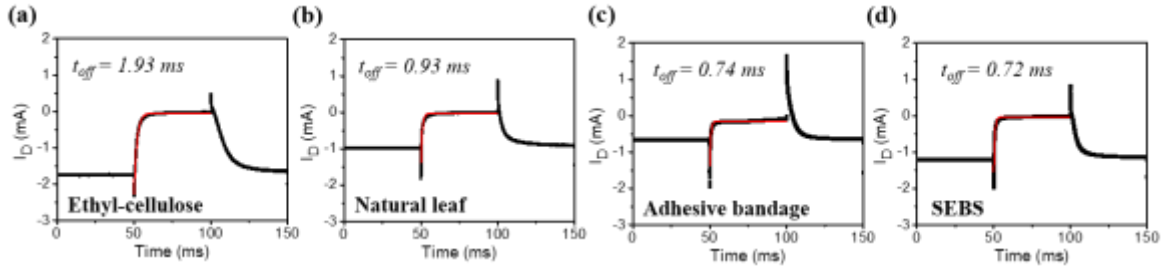

Figure S9. Stability study of OECTs on (a) biodegradable ethyl-cellulose-, (b) natural leaf-, (c) commercial adhesive bandage-, and (d) SEBS elastomer-based substrates through pulse measurements (V_G vary from -0.4 V to 0.6 V, pulse length = 0.5 s, V_D = -0.5 V) with over 200 cycles of continuous operation in 0.1 M NaCl electrolyte.

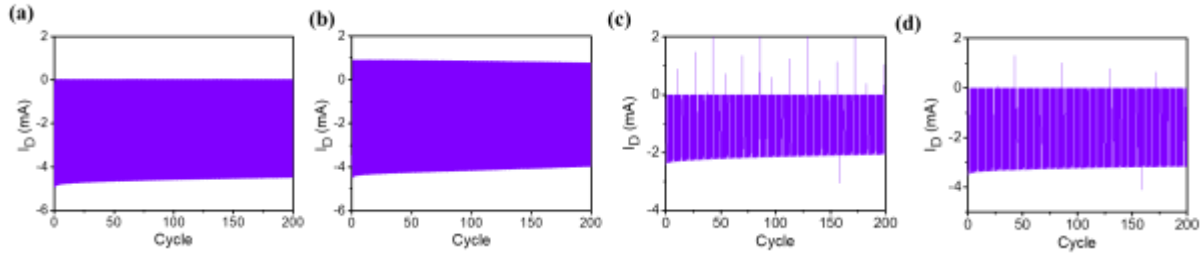

References

(1) Khodagholy, D.; Rivnay, J.; Sessolo, M.; Gurfinkel, M.; Leleux, P.; Jimison, L. H.; Stavrinidou, E.; Herve, T.; Sanaur, S.; Owens, R. M.; Malliaras, G.G. High Transconductance Organic Electrochemical Transistors. *Nat. Commun.* **2013**, *4*, 2133.

(2) Rivnay, J.; Leleux, P.; Ferro, M.; Sessolo, M.; Williamson, A.; Koutsouras, D. A.; Khodagholy, D.; Ramuz, M.; Strakosas, X.; Owens, R. M.; Benar, C. High-Performance Transistors for Bioelectronics through Tuning of Channel Thickness. *Sci. Adv.* **2015**, *1*, e1400251.

(3) Spyropoulos, G. D.; Gelinas, J. N.; Khodagholy, D. Internal Ion-Gated Organic Electrochemical Transistor: A Building Block for Integrated Bioelectronics. *Sci. Adv.* **2019**, *5*, eaau7378.